axial coordination. The Mo–Br distance of 2.879 (3) Å was substantially longer than the 2.604 (1) Å distance in $[Mo_2Br_8]^{4-}$ [16] or the 2.542 (1) and 2.545 (1) Å distances in $[Mo_2(O_2CCF_3)_2Br_4]^{2-}$. Similarly the Mo–I bonds at 3.180 (1) and 3.187 (1) Å were much longer than the ~2.78 Å observed in $[Mo_2I_6(H_2O)_2]^{2-}$.[18] This is in agreement with the very long Mo–N distance reported in the bis(pyridine) adduct.

The fluorine atoms in all the compounds reported were very anisotropic with extremely large temperature parameters. For this reason they have been omitted from Figures 2 and 3. This behavior, which is not uncommon for fluorine atoms on trifluoromethyl groups, can be attributed to rotation about the C–C bond resulting in the large thermal ellipsoids. This motion also resulted in large variations and errors in the C–F bond lenghts and C–C–F bond angles.

(18) (a) Brencic, J. V.; Segedin, P. *Inorg. Chim. Acta* **1978**, *29*, L287. (b) Brencic, J. V.; Golic, L. *J. Cryst. Mol. Struct.* **1977**, *7*, 183.

Registry No. $(N(n\text{-}Bu)_4)_2[Mo_2(O_2CCF_3)_4Br_2]$, 84987-30-4; $(N(n\text{-}Bu)_4)_2[Mo_2(O_2CCF_3)_4I_2]$, 84987-31-5; $(N(n\text{-}Bu)_4)_2[Mo_2(O_2CCF_3)_2Br_4]$, 7439-98-7.

Supplementary Material Available: Listings of bond distances and angles for the tetrabutylammonium cations (Table VIII), thermal parameters and their errors (Tables IX, X, and XI), and observed and calculated structure factors (Tables XII, XIII, and XIV) (59 pages). Ordering information is given on any current masthead page.

Contribution from the Department of Chemistry, University of Cincinnati, Cincinnati, Ohio 45221, and the Miami Valley Laboratories, Procter & Gamble Company, Cincinnati, Ohio 45239

Calcium Affinity of Coordinated Diphosphonate Ligands. Single-Crystal Structure of $[(en)_2Co(O_2P(OH)CH_2P(OH)O_2)]ClO_4 \cdot H_2O$. Implications for the Chemistry of Technetium-99m–Diphosphonate Skeletal Imaging Agents

SILVIA S. JURISSON,[1] JAMES J. BENEDICT,[2] R. C. ELDER,[1] R. WHITTLE,[1] and EDWARD DEUTSCH*[1]

Received August 2, 1982

A series of (diphosphonato)bis(ethylenediamine)cobalt(III) complexes, where the diphosphonate ligand has the formula $HO_3P–CR(R')–PO_3H^{2-}$, has been prepared. Members of the series include the following R/R′ combinations: H/H, H/CH_3, CH_3/CH_3, H/OH, CH_3/OH, phenyl/OH, *tert*-butyl/OH, H/NH_2, CH_3/NH_2, H/$N(CH_3)_2$, H/Cl, and Cl/Cl. The complexes have been characterized in all cases by visible–UV, IR, ^1H NMR, and ^{31}P NMR spectra, in several cases by elemental analyses, and for the prototype title complex (R/R′ = H/H) by single-crystal X-ray structural analysis refined to a conventional *R* factor of 0.034. Equilibrium constants governing the one-to-one association with calcium(II) in dilute aqueous solution (pH 10, NH_4OH/NH_4Cl buffer, μ = 0.1 M (KCl), 25 °C) have been determined potentiometrically for all diphosphonate complexes as well as for the analogous pyrophosphato and oxalato complexes. Values of the equilibrium constants for the H/OH, H/H, and CH_3/OH complexes are 2.4×10^6, 1.8×10^4, and 1.1×10^4 M^{-1}, respectively, showing (a) that coordinated diphosphonate ligands have considerable affinity for calcium(II) and (b) that when R′ = OH the calcium affinity is enhanced, presumably via coordination of this OH group to calcium and formation of a bidentate–tridentate bridge from cobalt to calcium. This ordering of affinities exactly parallels the ordering of skeletal uptake of these three diphosphonate ligands when labeled with ^{99m}Tc, implying that binding of Tc–diphosphonate complexes to calcium at the surface of bone is an important step in the mechanism of in vivo action of ^{99m}Tc–diphosphonate skeletal imaging agents.

Introduction

Diphosphonates are a class of ligands that are chemically related to, and mimic the physiological behavior of, pyrophosphate:

$O_3P–O–PO_3^{4-}$	$O_3P–CR(R')–PO_3^{4-}$
pyrophosphate	diphosphonate

Most importantly, both pyrophosphate and diphosphonate ligands have very high affinity for calcium(II) in homogeneous solution and at the surfaces of minerals and bone. However, for many physiological applications diphosphonates are superior to pyrophosphate in that (1) the P–CR(R′)–P linkage is much more resistant to hydrolysis than is the P–O–P linkage[3] and (2) by variation of the R and R′ groups of the diphosphonate backbone the chemical and biological properties of these ligands can be extensively modified. Simple diphosphonate salts are used therapeutically for the treatment of bone and calcium metabolic disorders,[4] but more importantly, diphosphonate complexes of technetium-99m are widely used as diagnostic agents.[5] These agents are referred to as radiopharmaceuticals because it is the γ-ray activity of the ^{99m}Tc that provides the diagnostic image.[6] ^{99m}Tc–diphosphonate radiopharmaceuticals accumulate at sites of high calcium metabolic activity such as those that occur in the skeleton or in areas of recently infarcted myocardium.[7] Very little is known about the in vivo mechanism of action of these clinically important agents, but it is generally thought to be the residual chemical affinity of the *coordinated* diphosphonate ligand of the technetium–diphosphonate complex that drives deposition of the radiopharmaceutical at sites of high calcium metabolic activity.[8] For this reason we sought to investigate the calcium affinity of *coordinated* diphosphonate (and pyrophosphate) ligands and especially to determine how calcium affinity varies with the nature of the R and R′ substituent groups. Also of interest is whether or not these chemical

(1) University of Cincinnati.
(2) Procter & Gamble Co.
(3) Francis, M. D.; Centner, R. L. *J. Chem. Educ.* **1978** *55*, 760–6.
(4) Khairi, M. A. A.; Meunier, P.; Edouard, C.; et al. *Calcif. Tissue Res.* **1977**, *22*, 355–8 (suppl.).
(5) (a) Tofe, A. J.; Francis, M. D. *J. Nucl. Med.* **1974**, *15*, 69–74. (b) Eckelman, W. C.; Levenson, S. M. *Int. J. Appl. Radiat. Isot.* **1977**, 28, 67–82. (c) Jones, A.; Francis, M. D.; Davis, M. A. *Semin. Nucl. Med.* **1976**, *6*, 3–18.
(6) Hayes, R. L. "The Chemistry of Radiopharmaceuticals"; Heindel, N. D.; Burns, H. D., Honda, T., Brady, L. W., Eds.; Masson: New York, 1978; pp 155–68.
(7) Francis, M. D.; Slough, C. L.; Tofe, A. J. *Calcif. Tissue Res.* **1976**, *20*, 303.
(8) Deutsch, E. "Radiopharmaceuticals II: Proceedings of the Second International Symposium on Radiopharmaceuticals"; Society of Nuclear Medicine: New York, 1979; pp 129–46.

0020-1669/83/1322-1332$01.50/0

Table I. Nomenclature and Acronyms

acronym	formula	name
H_4MDP	$H_2O_3PCH_2PO_3H_2$	methylenediphosphonic acid
H_4EDP	$H_2O_3PCH(CH_3)PO_3H_2$	ethylidenediphosphonic acid
H_4DMDP	$H_2O_3PC(CH_3)_2PO_3H_2$	propylidene-2,2-diphosphonic acid
Na_2H_2HMDP	$NaHO_3PCH(OH)PO_3HNa$	disodium (hydroxymethylene)diphosphate
Na_2H_2HEDP	$NaHO_3PC(CH_3)(OH)PO_3HNa$	disodium (1-hydroxyethylidene)diphosphonate
$Na_2H_2BuHMDP$	$NaHO_3PC(C(CH_3)_3)(OH)PO_3HNa$	disodium (*tert*-butylhydroxymethylene)diphosphonate
$Na_2H_2PhHMDP$	$NaHO_3PC(C_6H_5)(OH)PO_3HNa$	disodium (α-hydroxybenzyl)diphosphonate
NaH_3AMDP	$NaHO_3PCH(N^+H_3)PO_3^-H$	sodium (aminomethylene)diphosphonate
H_4AEDP	$H_2O_3PC(CH_3)(N^+H_3)PO_3^-H$	(1-aminoethylidene)diphosphonic acid
H_4Me_2NMDP	$H_2O_3PCH(N^+H(CH_3)_2)PO_3^-H\cdot H_2O$	((dimethylamino)methylene)diphosphonic acid hydrate
H_4ClMDP	$H_2O_3PCH(Cl)PO_3H_2$	(chloromethylene)diphosphonic acid
$Na_2H_2Cl_2MDP$	$NaHO_3PC(Cl)_2PO_3HNa$	disodium (dichloromethylene)diphosphonate
en	$H_2NCH_2CH_2NH_2$	ethylenediamine

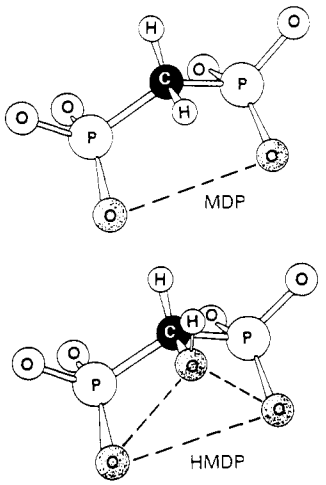

Figure 1. Bidentate and tridentate bonding modes shown for MDP^{4-} and $HMDP^{4-}$, respectively.

variations correlate with the physiological variations induced by varying R and R′ in technetium–diphosphonate radiopharmaceuticals. For example, when R = OH or some other potentially chelating functionality such as NH_2, the resulting technetium–diphosphonate skeletal imaging agents exhibit markedly different physiological properties than when R is a group such as H or CH_3 that cannot bind to calcium.[9] It has been proposed that these differences in physiological properties result from the ability of diphosphonates with potentially chelating R groups to form a bidentate–tridentate bridge from Tc to Ca, whereas diphosphonates with nonchelating R groups can form only bidentate–bidentate bridges[10] (Figure 1). This bridging, via increased denticity of diphosphonates containing potentially chelating R groups, should be reflected in the coordinated diphosphonate ligand having a higher affinity for calcium(II).

The chemical nature of the ^{99m}Tc–diphosphonate radiopharmaceuticals used for skeletal imaging is largely unknown.[5c] Moreover, the coordination chemistry of technetium is not sufficiently developed to provide a core complex that can be systematically modified by varying diphosphonate ligands (the only well-characterized ^{99}Tc–diphosphonate complex is polymeric in the solid state[10]). In light of these difficulties we have utilized the bis(ethylenediamine)cobalt(III) core to generate a series of well-characterized, substitution-inert, diphosphonate complexes: $[(en)_2Co(O_3PCR(R')PO_3)]^-$. These materials are not intended to be models for technetium–diphosphonate radiopharmaceuticals but rather are well-defined chemical probes for assessing the extent of interaction between calcium(II) and coordinated diphosphonate ligands. In this paper we report on the synthesis and characterization of these probe complexes, including a single-crystal X-ray structural analysis of the prototype title complex, and on the affinity of these complexes for calcium(II) in dilute aqueous media.

Nomenclature

Specific nomenclature and acronyms used in identifying ligands and complexes are given in Table I.

Experimental Section

General Comments. All common laboratory chemicals were of reagent grade. H_4MDP, Na_2H_2HMDP, Na_2H_2HEDP, $H_4PhHMDP$, $Na_2H_2BuHMDP$, H_4Me_2NMDP, H_4ClMDP, and $Na_2H_2Cl_2MDP$ were available from previous studies. H_4EDP, H_4DMDP, and H_4AEDP were purchased from the Alfa Division of Ventron Corp. All diphosphonate ligands were used as received and except for H_4ClMDP and H_4EDP were shown to be >90% pure by ^{31}P NMR. H_4ClMDP was contaminated with H_4Cl_2MDP and H_4MDP and by ^{31}P NMR analysis was only ca. 80% pure; H_4EDP was contaminated with H_4DMDP and H_4MDP and by ^{31}P NMR analysis was only ca. 80% pure. Elemental analyses were performed by Galbraith Laboratories, Inc., Knoxville, TN, while total cobalt analysis of solutions and solid samples was performed by a modified Kitson procedure.[11,12] Dowex 50W-X2 cation-exchange resin was cleaned as previously described,[13] while Sephadex SP-C25 cation exchanger was prepared and stored according to the manufacturer's (Pharmacia, Inc.) directions.

Materials. *cis*-Dichlorobis(ethylenediamine)cobalt(III) chloride and **tris(ethylenediamine)cobalt(III) chloride** were prepared according to literature procedures.[14]

Sodium (Aminomethylene)diphosphonate, NaH_3AMDP. H_4AMDP was prepared by a literature procedure[15] and converted to the sodium salt by adjusting the pH of an aqueous solution to 6 with 1 N NaOH. This salt was recovered by precipitation with methanol and shown to be >90% pure by ^{31}P NMR.

(Diphosphonato)bis(ethylenediamine)cobalt(III) Perchlorate Salts. All the compounds listed in Table II were prepared similarly. The following is a typical preparation of [(1-hydroxyethylidene)diphosphato]bis(ethylenediamine)cobalt(III) perchlorate dihydrate, $[(en)_2Co(H_2HEDP)]ClO_4\cdot 2H_2O$. One gram (3.5 mmol) of *cis*-$[(en)_2CoCl_2]Cl$ was dissolved in 15 mL of water on a water bath at 70–80 °C, and 0.9 g (3.6 mmol) of Na_2H_2HEDP in 10 mL of water was added to this solution (when the acid form of a diphosphonate ligand was used, the pH was first adjusted to ca. 7 with 1 N NaOH). The solution became deep red as the reaction proceeded. The reaction solution was concentrated for 1–2 h on the water bath to approximately half its original volume. The solution was cooled, acidified with dilute (0.025–0.1 N) $HClO_4$, and purified by cation-exchange chromatog-

(9) Deutsch, E.; Barnett, B. L. "Inorganic Chemistry in Biology and Medicine"; Martell, A. E., Ed.; American Chemical Society: Washington, DC, 1980; ACS Symp. Ser. No. 140, pp 130–46.
(10) Libson, K.; Deutsch, E.; Barnett, B. L. *J. Am. Chem. Soc.* **1980**, *102*, 2476–8.
(11) Kitson, R. E. *Anal. Chem.* **1950**, *22*, 664.
(12) Hughes, R. G.; Endicott, J. F.; Hoffmann, M. Z.; House, D. A. *J. Chem. Educ.* **1969**, *46*, 440.
(13) Deutsch, E.; Taube, H. *Inorg. Chem.* **1968**, *7*, 532.
(14) Schlessinger, G. G. "Inorganic Laboratory Preparations"; Chemical Publishing Co.: New York, 1962: (a) pp 237–8; (b) pp 186–8.
(15) Ploger, W.; Schlindler, N.; Wollman, K.; Worms, K.-H. *Z. Anorg. Allg. Chem.* **1972**, *389*, 119–28.

Table II. Calcium Binding Constants of $[(en)_2Co(O_3PCR(R')PO_3)]^-$ Complexes[a,b]

class or series	complex	R	R'	K, M^{-1}
alkyl	MDP	H	H	$1.8\ (1) \times 10^4$
	EDP[d]	H	CH_3	$4.6\ (1) \times 10^3$
	DMDP	CH_3	CH_3	$3.6\ (1) \times 10^3$
hydroxyl	HMDP	OH	H	$2.4\ (5) \times 10^6$
	HEDP	OH	CH_3	$1.1\ (1) \times 10^4$
	PhHMDP	OH	phenyl	$6.2\ (3) \times 10^3$
	BuHMDP	OH	*tert*-butyl	$4.8\ (3) \times 10^3$
amine	AMDP	NH_2	H	$9.7\ (7) \times 10^3$
	AEDP	NH_2	CH_3	$2.0\ (1) \times 10^4$
	Me_2NMDP	$N(CH_3)_2$	H	$1.1\ (1) \times 10^4$
chloro	ClMDP[d]	Cl	H	$4.6\ (3) \times 10^3$
	Cl_2MDP	Cl	Cl	$4.4\ (3) \times 10^3$
other	pyrophosphate[e]			10^3 [c]
	oxalate[f]			200[c]

[a] Conditions: 25.0 °C, pH 10, μ = 0.1 M (KCl). Standard deviations of the last digits are given in parentheses. This form is used throughout. [b] Ca^{2+} + Co-diP$^-$ ⇄ Co-diP-Ca$^+$; K = [Co-diP-Ca$^+$]/([Ca^{2+}][Co-diP$^-$]. [c] These complexes slowly hydrolyze during the course of the titration, and thus the quoted approximate values of K are obtained with use of data from the early portion of the titration. [d] These complexes contain a mixture of diphosphonate ligands (vide infra). [e] Seel, V. F.; Bohnstedt, G. *Z. Anorg. Allg. Chem.* **1978**, *441*, 237–44. [f] Mathieu, J.-P. In "Gmelins Handbuch der Anorganische Chemie"; Kobalt Teil B; Kotowski, A., Ed.; Springer-Verlag: West Berlin, 1964; Cobalt Vol. B, p 539.

raphy on Dowex 50W-X2 with 1 and 2 N $HClO_4$ eluents for 1+ and 2+ charged complexes, respectively. (For complexes containing phenyl substituents, Sephadex SPC-25 cation-exchange resin was used with $NaClO_4$/0.025 N $HClO_4$ as the eluent.) Several bands were observed during the ion-exchange separation. In order of elution, the first band was green, unreacted *trans*-$[(en)_2CoCl_2]^+$ (3–5% based on Co), which was followed by a ruby red band containing the diphosphonate complex (usually 80–90% yield) and then a few highly retained bands that remained near the top of the column (5–10% yield). The diphosphonate complex was obtained as the perchlorate salt by allowing the solvent to evaporate at room temperature or by concentrating the solution by vacuum rotary evaporation and then inducing precipitation with *sec*-butyl alcohol and ethyl ether at −10 °C. In either case, the solid product was collected by suction filtration and washed with 95% ethanol. The only exception to this general procedure was in the case of the BuHMDP complex. Na_2H_2BuHMDP is not very soluble at pH 7, and no attempts were made to totally dissolve the ligand before adding it to the reaction vessel. $[Co(en)_2(H_2BuHMDP)]^+$ was not chromatographically purified since the complex precipitated as the perchlorate salt immediately upon addition of dilute (~0.1 N) perchloric acid.

The visible–UV, ^{1}H NMR, and ^{31}P NMR spectral parameters observed for these complexes are given in Tables A, B, and C,[16] respectively. All complexes were analyzed for total cobalt content while C, H, N, Cl, and P analyses were obtained for the H_2HEDP^{2-}, H_3AMDP^-, and $H_2Cl_2MDP^{2-}$ complexes; these data are given in Table D.[16]

Equipment. Visible–UV spectra were recorded on a Cary Model 210 spectrophotometer at ambient temperature and in aqueous solution. Infrared spectra were obtained in KBr pellets with a Perkin-Elmer Model 599 spectrometer. ^{1}H NMR spectra were recorded in aqueous media (pH 1–2), with DSS as an internal standard, on a Varian T-60 spectrometer. ^{31}P NMR spectra were recorded in aqueous media (pH 0.5–12.5), with 85% H_3PO_4 as an external standard, on a JEOL Model FX90Q pulsed Fourier transform 90-MHz spectrometer. Data defining the equilibrium between calcium(II) and the diphosphonate–cobalt complexes were obtained with an Orion Model 93-20 calcium ion electrode, an Orion Model 90-02 double-junction (Ag/AgCl) reference electrode, and a Beckman Research pH meter; all samples were maintained at 25.0 ± 0.2 °C with a Haake-FT temperature bath.

Equilibrium Measurements. Stock solutions of Ca(II) were prepared with use of $CaCO_3$, concentrated HCl, and degassed, doubly distilled water. After further degassing to remove CO_2, the concentration of calcium(II) in the stock solution was determined by titration with a standardized EDTA solution (Fisher Scientific Co.) and Eriochrome Black T as an indicator. Solutions of calcium(II) and solutions of the diphosphonate–cobalt(III) complexes were brought to ionic strength 0.1 M with KCl and adjusted to pH 10 (NH_4OH/NH_4Cl buffer) for the equilibrium measurements. The calcium ion electrode was calibrated prior to each equilibrium determination with use of diluted calcium stock solutions (10^{-1}–10^{-6} M) brought to the same conditions as the test solutions. During these calibrations a 10-fold increase in calcium(II) concentration gave approximately a 27–30-mV increase in electrode potential. The equilibrium measurements were determined by titrating the diphosphonate–cobalt(III) solution into the calcium(II) solution, electrode potential measurements being taken once equilibrium was reestablished after each addition of the diphosphonate–cobalt(III) solution. The concentration of cobalt(III) in the titrant was more than 10 times greater than the concentration of calcium in order to minimize dilution effects. The resulting EMF vs. volume data were used to determine the apparent equilibrium constant, K, governing association of calcium(II) with the diphosphonate–cobalt(III) complex. Values of K, defined as

$$K = \frac{[\text{Co–diphosphonate–Ca}^+]}{[\text{Ca}^{2+}][\text{Co–diphosphonate}^-]}$$

were calculated by nonlinear regression analysis[17] within the expression

$$E = A + B(\log [\text{Ca}^{2+}]_0)V_0/(KLV + V + V_0) \qquad (1)$$

where $[Ca^{2+}]_0$ and V_0 are the initial concentration and volume of the calcium solution, respectively, L and V are the concentration and volume added of the diphosphonate–cobalt(III) solution, respectively, A and B are the y intercept and slope of the calcium ion electrode calibration plot (mV vs. log [Ca^{2+}]), respectively, and E is the electrode potential in mV. The resulting values of K and the associated standard deviations, σ_K, are given in Table II. Replicate determinations showed that K values obtained in this manner were reproducible on the average to ±6% and in the worst case to ±15%.

X-ray Structure Characterization of $[(en)_2Co(H_2MDP)]ClO_4 \cdot 2H_2O$. A large red crystal with a parallelepiped morphology was mounted on a glass fiber, and precession photographs of the *hk*0, 0*kl*, and *hkl* layers, taken with use of Cu Kα radiation, indicated that the crystal was of the triclinic class. A crystal of similar morphology (0.25 × 0.15 × 0.10 mm) was mounted on a glass fiber and optically centered on a Syntex P$\bar{1}$ diffractometer. Precise cell constants were determined by least-squares refinement using 2θ values of 15 pairs of reflections measured at $+2\theta$ and -2θ values in the range of 21–29°. The cell constants for the reduced primitive cell are a = 8.860 (2) Å, b = 9.272 (2) Å, c = 12.137 (4) Å, α = 88.88 (2)°, β = 73.14 (2)°, and γ = 68.19 (2)°. With Z = 2, the calculated density is 1.84 g cm^{-3}; the measured density is 1.84 (3) g cm^{-3} (neutral buoyancy in CCl_4/$CHBr_3$). All measurements were at room temperature.

Intensity measurements were made as previously described[18] for the 2985 reflections with $2\theta < 45°$ and h ranging from 0 to +9, k from +10 to −9, and l from +13 to −13. From these data 2630 unique reflections were obtained. The θ–2θ scan for these measurements, with Mo Kα radiation (λ = 0.710 69 Å) and a graphite monochromator, was from 0.6° below to 0.6° above the reflection in 2θ. Scan rates varied from 2.0 to 8.0° min^{-1} depending on the intensity of the reflection. The four standard reflections, which were monitored to check stability and account for long-term drift, varied a maximum of ±1.5%, and the drift was random. Thus, no rescaling corrections were used. The linear absorption coefficient, μ, was 13.52 cm^{-1}, generating a maximum estimated error in F of 2.3%, and thus no absorption corrections were applied. Of the set of 2630 unique, normalized structure factors, 2466 had $F_o^2 > 2\sigma(F_o^2)$, where a value of 0.02 was used for P, the ignorance factor,[18] in calculating $\sigma(F_o^2)$.

A Patterson map[19] was computed, and the positions of the cobalt atom, the two phosphorus atoms, and the chlorine atom were de-

(16) Supplementary material.

(17) Moore, R. H.; Ziegler, R. K. *Los Alamos Sci. Lab.* [*Rep.*] *LA* **1959**, *LA-2367* (plus addenda).
(18) Elder, R. C.; Florian, L. R.; Lake, R. E.; Yacynych, A. M. *Inorg. Chem.* **1973**, *12*, 2690–9.
(19) All computations were performed by using a local version of X-RAY 67: Stewart, J. M., Crystallographic Computer System, University of Maryland.

termined in agreement with the space group $P\bar{1}$. An electron density synthesis based on the signs derived from these four atom positions revealed the remaining 21 non-hydrogen atoms. Least-squares refinement of atom positions, general scale factors, and isotropic thermal parameters gave $R_1 = 0.084$.[20] Refinement of the model was continued with anisotropic thermal parameters. The positions of the 24 hydrogen atoms were determined from the electron density map through continued refinement (all hydrogen atoms were assigned isotropic thermal parameters[21] of $B = 4.0$ Å^2). Full-matrix refinement of the non-hydrogen atom positions, their temperature factors, and the hydrogen atom positions converged to $R_1 = 0.034$ and $R_2 = 0.034$.[22] The 2630 structure factors were used to refine 298 variables. In the final cycle of refinement, the maximum shift per error was 0.14 and the average shift per error was 0.022. A final difference electron density map consisted of five unidentified peaks of height greater than 0.14 e Å^{-3}. The two peaks of highest intensity (0.24 e Å^3) were both in the region of the perchlorate anion. Scattering curves were taken from standard tabulations[23,24] for P, Co, O, N, Cl, C, and H. Corrections for anomalous dispersion[24] were made by using $\Delta f'$ and $\Delta f''$ values of 0.299 and 0.973 for Co, 0.09 and 0.095 for P, and 0.132 and 0.159 for Cl. The values of $|F_o|$ and F_c are listed in Table E.[16]

Results

Characterization. In addition to the X-ray structural analysis described below, the diphosphonate cobalt(III) complexes are characterized by (a) the synthetic route employed for their preparation, (b) elemental analyses (and/or total cobalt analyses), which give empirical compositions in agreement with those predicted (Table D),[16] (c) cation-exchange elution characteristics, which are consistent with the assigned formal charges, (d) infrared spectral data, and (e) the visible–UV, ^{1}H NMR, and ^{31}P NMR spectral parameters, which are listed in Tables A, B, and C,[16] respectively.

While all the complexes prepared are clearly of the form $[(en)_2Co(diphosphonate)]^-$, those materials prepared from impure diphosphonate ligands naturally contain a mixture of diphosphonate complexes. The "monochloro" and "monomethyl" ligands (H_4ClMDP and H_4EDP) are contaminated respectively with the "dichloro" and "dimethyl" analogues (H_4Cl_2MDP and H_4DMDP) as well as with the unsubstituted analogue H_4MDP. Thus, $[(en)_2Co(ClMDP)]^-$ is only about 80% pure, being contaminated with $[(en)_2Co(Cl_2MDP)]^-$ and $[(en)_2Co(MDP)]^-$, and $[(en)_2Co(EDP)]^-$ is only about 80% pure, being contaminated with $[(en)_2Co(DMDP)]^-$ and $[(en)_2Co(MDP)]^-$.

The visible–UV spectra of these complexes are characteristic of the *cis*-$N_4O_2Co^{III}$ chromophore. Two d–d transitions are observed at ca. 510 and ca. 370 nm, which arise from the $^1A_{1g} \rightarrow {}^1T_{1g}$ and $^1A_{1g} \rightarrow {}^1T_{2g}$ transitions, respectively. For example, the visible–UV spectrum of $[Co(en)_2(OH_2)(HPO_4)]^+$ exhibits maxima at 511 and 366 nm,[26] while that of $[(en)_2Co(H_2MDP)]^+$ exhibits maxima at 510 and 369 nm (Table A).[16]

The infrared spectra of the complexes are very similar and are dominated by the P=O (1000–1200 cm^{-1}), ClO_4^- and N–H (3500 and 1600 cm^{-1}) signals.

The ^{1}H NMR spectra of the diphosphonate–cobalt(III) complexes confirm the presence and nature of the diphosphonate ligand. The two phosphorus atoms ($I = {}^1/_2$) of the diphosphonate ligand couple ($J_{P-H} \cong 15$–20 Hz) with protons bonded to the α- and β-carbon atoms of this ligand. The chemical shifts associated with protons of the R and R′ groups of the geminal carbon atom are dependent on the nature of the three other functionalities bonded to this carbon atom (Table B).[16] The coordinated ethylenediamine resonances appear as would be expected: $-CH_2CH_2$, 2.8 ppm, multiplet; trans-NH_2, 4.3 ppm, broad; cis-NH_2, 5.85 ppm, broad; integration ratio 2:2:1.

The proton-decoupled ^{31}P NMR spectra of these complexes exhibit a singlet for those diphosphonate–cobalt(II) complexes in which the R and R′ groups are identical. When R and R′ are different, an AB pattern is observed (Table C[16] and Figure 2). As expected, the deshielding effect of the positively charged cobalt(III) center causes the chemical shifts of the coordinated ligands to appear ca. 10 ppm downfield from those of the noncoordinated ligands. The proton-coupled ^{31}P NMR spectra also exhibit J_{P-H} values of 15–20 Hz.

Equilibrium Measurements. The results of the calcium equilibrium studies are given in Table II. Measurements were conducted at pH 10 since at this pH the calcium ion electrode has maximum sensitivity and the cobalt(III) complexes are essentially deprotonated and reasonably soluble.

Application of Job's method[27] for spectrophotometrically determining the ratio of reactants involved in an equilibrium yields a calcium:diphosphonate–Co(III) ratio of 1.0. This

Table III. Fractional Atomic Positional Parameters[a,b] for $[(en)_2Co(H_2MDP)]ClO_4 \cdot 2H_2O$

atom	x	y	z
Co	0.0178 (1)	0.34964 (4)	0.21627 (3)
P(1)	0.1585 (2)	0.5540 (1)	0.3337 (1)
P(2)	0.2754 (2)	0.4899 (1)	0.0711 (1)
O(1)	0.0321 (3)	0.4819 (3)	0.3306 (2)
O(2)	0.0856 (4)	0.6887 (3)	0.4240 (2)
O(3)	0.3244 (4)	0.4274 (3)	0.3482 (3)
O(4)	0.3067 (3)	0.5742 (3)	−0.0358 (2)
O(5)	0.4364 (4)	0.3423 (3)	0.0692 (3)
O(6)	0.1308 (3)	0.4342 (3)	0.0862 (2)
N(1)	0.2321 (4)	0.1773 (3)	0.2118 (3)
N(2)	0.0014 (5)	0.2151 (4)	0.1037 (3)
N(3)	−0.1155 (4)	0.2793 (4)	0.3450 (3)
N(4)	−0.1977 (4)	0.5143 (3)	0.2195 (3)
C(1)	0.2826 (6)	0.0603 (5)	0.1116 (4)
C(2)	0.1212 (6)	0.0518 (4)	0.1007 (4)
C(3)	−0.3002 (5)	0.3634 (5)	0.3614 (4)
C(4)	−0.3264 (5)	0.5276 (4)	0.3330 (3)
C(5)	0.2317 (5)	0.6186 (4)	0.1954 (3)
Cl	0.7093 (2)	0.9566 (1)	0.2459 (1)
O(7)	0.6606 (5)	1.0890 (3)	0.1855 (3)
O(8)	0.7763 (7)	0.9926 (4)	0.3308 (4)
O(9)	0.5759 (6)	0.9120 (5)	0.3023 (5)
O(10)	0.8397 (5)	0.8304 (3)	0.1692 (3)
O(11)	0.2597 (5)	0.2073 (3)	0.4662 (2)
O(12)	0.1483 (7)	−0.0434 (5)	0.3790 (3)

[a] The estimated errors in the last digits are shown in parentheses. This form is used throughout. [b] The numbering is as shown in Figure 4.

Table IV. Selected Bond Lengths (Å) for $[(en)_2Co(H_2MDP)]ClO_4 \cdot H_2O$

Co–N(1)	1.962 (3)	Co–N(4)	1.942 (3)
Co–N(2)	1.939 (4)	Co–N(3)	1.930 (3)
Co–O(1)	1.931 (3)	Co–O(6)	1.931 (2)
P(1)–O(1)	1.511 (3)	P(2)–O(6)	1.514 (3)
P(1)–O(2)	1.491 (2)	P(2)–O(4)	1.511 (2)
P(1)–O(3)	1.559 (3)	P(2)–O(5)	1.562 (2)
P(1)–C(5)	1.793 (3)	P(2)–C(5)	1.799 (4)
N(1)–C(1)	1.494 (5)	N(2)–C(2)	1.485 (4)
N(3)–C(3)	1.481 (5)	N(4)–C(4)	1.484 (4)
C(1)–C(2)	1.504 (7)	C(3)–C(4)	1.502 (5)
Cl–O(7)	1.409 (3)	Cl–O(8)	1.429 (6)
Cl–O(9)	1.385 (5)	Cl–O(10)	1.409 (2)

(20) $R_1 = \sum||F_o| - |F_c||/\sum|F_o|$.
(21) Isotropic thermal parameters were of the form $\exp(-B(\sin^2\theta)/\lambda^2)$.
(22) $R_2 = [\sum w(|F_o| - |F_c|)^2/w(F_o)^2]^{1/2}$.
(23) Cromer, D. T.; Mann, J. B. *Acta Crystallogr., Sect. A* **1968**, *A24*, 321–4.
(24) Stewart, R. F.; Davidson, E. R.; Simpson, W. T. *J. Chem. Phys.* **1965**, *42*, 3175–87.
(25) Ibers, J. A.; Hamilton, W. C. "International Tables for X-Ray Crystallography"; Kynoch Press: Birmingham, England, 1974; Vol. IV, pp 148–50.
(26) Lincoln, S. F.; Stranks, D. R. *Aust. J. Chem.* **1968**, *21*, 37–56.
(27) Skoog, D. A.; West, D. M. "Principles of Instrumental Analysis"; Holt, Rinehart and Winston: New York, 1971; pp 104–5.

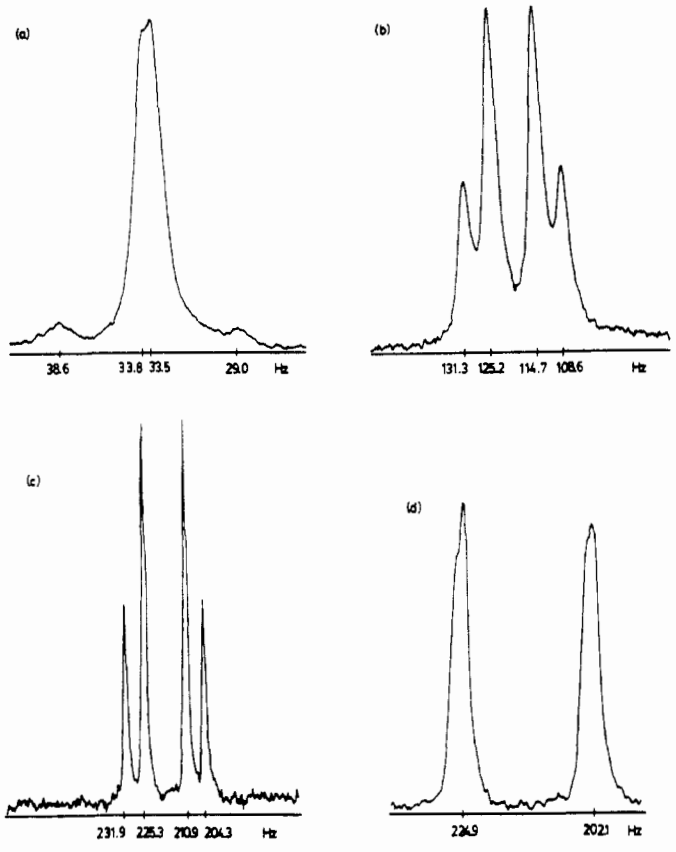

Figure 2. ^{31}P NMR spectra of $[(en)_2Co(H_3AMDP)]^{2+}$ in D_2O/DCl or D_2O/NaOD (85% H_3PO_4 external standard, ^1H decoupled) under the following pH conditions: (a) 1.6; (b) 4.1; (c) 6.9; (d) 10.4.

result, in conjunction with the successful refinement of the titration data within eq 1, demonstrates that the equilibrium between Ca(II) and the diphosphonate–cobalt(III) complexes may be adequately expressed as

$$Ca^{2+} + DiP\text{–}Co^{-} \rightleftarrows Ca\text{–}DiP\text{–}Co^{+}$$

Crystal Structure of $[(en)_2Co(H_2MDP)]ClO_4 \cdot 2H_2O$. Final fractional atomic coordinates and the associated estimated standard deviations for non-hydrogen atoms are listed in Table III. Anisotropic thermal parameters are listed in Table F.[16] The root mean square displacements are given in Table G.[16] Bond lengths and angles not involving hydrogen atoms are given in Tables IV and V, respectively. The final hydrogen atom fractional atomic coordinates and the associated estimated standard deviations are listed in Table H.[16] The bond lengths and angles involving hydrogen atoms are given in Tables I and J, respectively.[16] Possible hydrogen bonds are listed in Table K.[16]

Table V. Selected Bond Angles (deg) for $[(en)_2Co(H_2MDP)]ClO_4 \cdot 2H_2O$

Metal Coordination Sphere			
O(1)-Co-O(6)	94.3 (1)	O(1)-Co-N(1)	94.4 (2)
O(1)-Co-N(3)	86.1 (2)	O(1)-Co-N(4)	87.5 (2)
O(6)-Co-N(1)	92.2 (1)	O(6)-Co-N(2)	86.7 (2)
O(6)-Co-N(4)	88.9 (1)	N(1)-Co-N(2)	85.6 (2)
N(1)-Co-N(3)	93.2 (2)	N(2)-Co-N(3)	92.8 (2)
N(2)-Co-N(4)	92.5 (2)	N(3)-Co-N(4)	85.7 (2)
Ligands			
Co-N(1)-C(1)	109.6 (3)	Co-N(2)-C(2)	110.2 (3)
Co-N(3)-C(3)	110.5 (3)	Co-N(4)-C(4)	109.3 (2)
N(1)-C(1)-C(2)	107.1 (3)	N(2)-C(2)-C(1)	106.7 (4)
N(3)-C(3)-C(4)	107.2 (4)	N(4)-C(4)-C(3)	106.1 (3)
O(1)-P(1)-C(5)	109.7 (2)	O(6)-P(2)-C(5)	109.9 (2)
O(1)-P(1)-O(2)	112.9 (2)	O(6)-P(2)-O(4)	113.4 (2)
O(1)-P(1)-O(3)	110.4 (2)	O(6)-P(2)-O(5)	106.4 (2)
O(2)-P(1)-O(3)	111.3 (2)	O(4)-P(2)-O(5)	111.8 (2)
O(2)-P(1)-C(5)	108.8 (2)	O(4)-P(2)-C(5)	108.5 (2)
O(3)-P(1)-C(5)	103.3 (2)	O(5)-P(2)-C(5)	106.7 (2)
P(1)-C(5)-P(2)	116.1 (3)		
Anion			
O(7)-Cl-O(8)	108.0 (3)	O(7)-Cl-O(9)	113.7 (3)
O(7)-Cl-O(10)	109.8 (2)	O(8)-Cl-O(9)	108.0 (3)
O(8)-Cl-O(10)	108.1 (3)	O(9)-Cl-O(10)	109.2 (3)

The structure consists of $[(en)_2Co(O_2P(OH)CH_2P(OH)O_2)]^+$ cations, perchlorate anions, and waters of hydration. One water molecule is strongly hydrogen bonded to the hydrogen atom of a diphosphonate hydroxyl group while a second water molecule is hydrogen bonded to an amine hydrogen atom (Table K).[16] As shown in Figure 4, the complex is approximately octahedral with two bidentate ethylenediamine ligands and a bidentate methylenediphosphonate

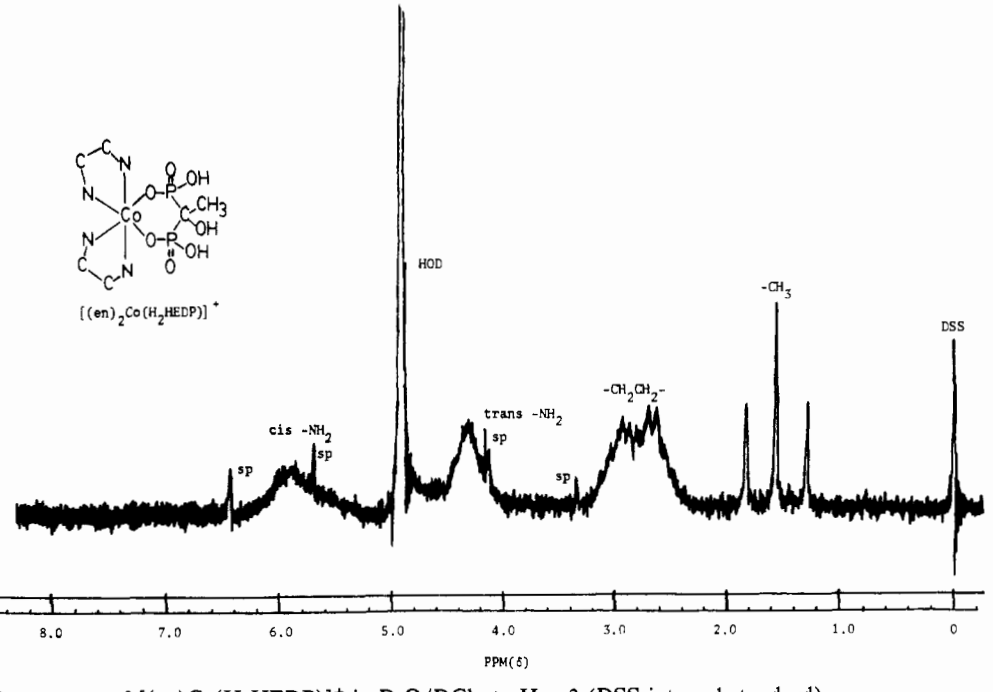

Figure 3. ^1H NMR spectrum of $[(en)Co(H_2HEDP)]^+$ in D_2O/DCl at pH ~2 (DSS internal standard).

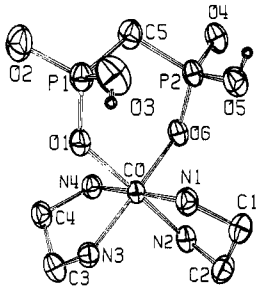

Figure 4. Perspective ORTEP drawing of the cation. Hydrogen atoms are omitted for clarity.

ligand. The methylenediphosphonate ligand is coordinated to the cobalt center through an oxygen atom from each phosphonate group to form a six-membered ring. This ring is somewhat distorted from a true chair conformation by the restraints of the approximately 90° O(1)–Co–O(6) angle. The plane defined by O(1), P(1), and O(3) of one PO_3 group is virtually parallel to the plane defined by O(6), P(2), and O(5) of the other PO_3 group. The O(3)–O(5) distance of the diphosphonate moiety is 3.23 Å, whereas the O(2)–O(4) distance is 5.33 Å. The O(3) and O(5) atoms are thus in a configuration wherein chelate coordination to Ca(II) could readily occur. Of course, in solution the configuration of the diphosphonate ring is expected to be flexible and the O(3)–O(5) distance will vary to accommodate different bonding modes.

Discussion

Synthesis and Characterization. The (diphosphonato)bis(ethylenediamine)cobalt(III) complexes are simply prepared by substitution of the diphosphonate ligand onto $[(en)_2CoCl_2]^+$. These complexes are stable over the pH range 0–12, but in the pH range 3–8 they are neutral and concomitantly only slightly soluble in water.

The ^1H NMR and ^{31}P NMR spectra of the diphosphonate–cobalt(III) complexes show phosphorus–proton coupling for the protons on the carbon atoms α and β to the phosphonate groups. When the two groups on the geminal carbon atom of the diphosphonate ligand are identical (R = R′), the ^{31}P NMR spectrum consists of a sharp singlet, indicating that the two phosphorus atoms are chemically equivalent. However, when the two groups on the geminal carbon are different (R ≠ R′), the phosphorus atoms are nonequivalent as evidenced by the observed phosphorus–phosphorus coupling. The coupling constants (J_{P-P}) of these AB "quartets" show substantial dependence on pH (Figure 2).

The structure of $[(en)_2Co(O_2P(OH)CH_2P(OH)O_2)]^+$ is typical of cobalt(III) complexes containing three bidentate ligands. The diphosphonate moiety is complexed to the cobalt center in a manner consistent with the strong chelating ability of this ligand and the reported structures of various sodium(I) and calcium(II) diphosphonate salts.[10,28-30] The bond angles and distances involving the methylenediphosphonate ligand agree very well with those observed in a polymeric technetium–methylenediphosphonate complex,[10] the most closely related material that has been structurally characterized.

A significant structural feature is the orientation of the PO_3 groups with respect to the P–C–P plane. A planar "W" configuration involving the atoms O(2)–P(1)–C(5)–P(2)–O(4) occurs (Figure 4) and has been previously described.[29,30] This configuration allows the ligand to be doubly bidentate with O(1) and O(6) coordinated to the cobalt on one side of the "W" and O(3) and O(5) capable of complexing another metal on the other side of the "W". This doubly bidentate character[10] allows the diphosphonate ligand to bridge the cobalt(III) center to calcium(II).

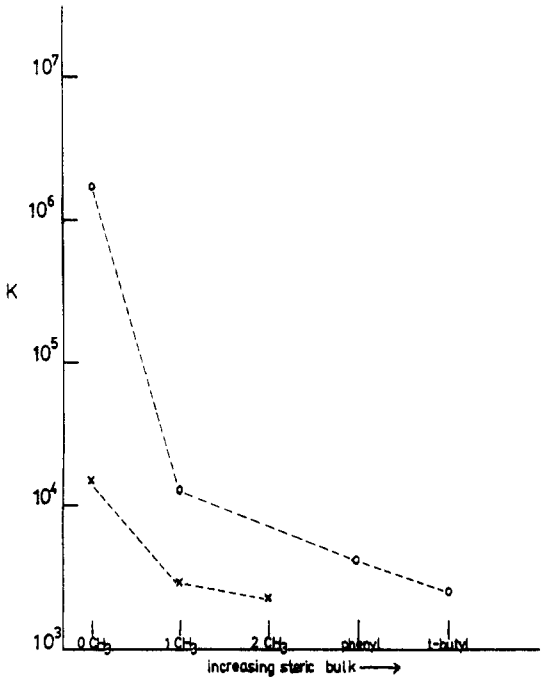

Figure 5. Variation of calcium binding constants, K, with increasing steric bulk for two series of $[(en)_2Co(O_3PCR(R')PO_3)]^-$ complexes. Circles represent the R/R′ combinations H/OH, CH_3/OH, phenyl/OH, and *tert*-butyl/OH, while crosses represent the R/R′ combinations H/H, H/CH_3, and CH_3/CH_3.

Calcium Affinity. Values of the apparent equilibrium constants, K, governing the association of calcium(II) with the coordinated diphosphonates (pH = 10, μ = 0.1 M (KCl), 25 °C) are given in Table II. Since the calcium affinity of $[(en)_3Co]^{3+}$ is undetectably small under these conditions, the observed K values are not influenced by the coordinated ethylenediamine ligands but are determined solely by the nature of the coordinated diphosphonate ligand. These K values are large, ranging from 4×10^3 to 2×10^6 M^{-1}, showing that even after coordination the diphosphonate ligand has considerable affinity for calcium. In fact, all the complexes in Table II have greater calcium affinities than does free oxalate ($K = 10^3$ M^{-1} under comparable conditions).[31] As expected, the calcium affinity of a coordinated diphosphonate is significantly less than (ca. 50-fold) that of a noncoordinated diphosphonate, comparable K values for coordinated and noncoordinated MDP^{4-} being 1.8×10^4 and 1×10^6 M^{-1},[32] respectively. Similarly, coordination of oxalate to the bis(ethylenediamine)cobalt(III) center reduces its calcium affinity by about 50-fold, i.e. from 1×10^3[31] to ca. 200 M^{-1}.

The data of Table II show that the calcium affinity of a given coordinated diphosphonate ligand (O_3P–C(R)(R′)–PO_3^{4-}) depends strongly on the nature of the R and R′ groups. The observed variations are conveniently classified as resulting from steric effects, electronic effects, and chelate effects.

(a) Steric Effects. Increasing the steric bulk of the R and R′ groups of the coordinated diphosphonate ligand reduces the observed value of K (Table II). Figure 5 illustrates this effect for two series of analogous complexes. The most dramatic changes occur upon replacing a single H group by a CH_3

(28) Uchtman, V. A.; Gloss, R. A. *J. Phys. Chem.* **1972**, *76*, 1298–1304.
(29) Uchtman, V. A. *J. Phys. Chem.* **1972**, *76*, 1304–10.
(30) Barnett, B. L.; Strickland, L. C. *Acta Crystallogr., Sect. B* **1979**, *B35*, 1212–4.
(31) Sillen, L. G.; Martell, A. E. "Stability Constants of Metal-Ion Complexes"; Chemical Society: London, 1964; p 360.
(32) Irani, R. R.; Moedritzer, K. *J. Phys. Chem.* **1962**, *66*, 1349–53.

group, K decreasing by a factor of 4 on going from R/R′ = H/H to R/R′ = H/CH_3 and a factor of 200 on going from R/R′ = H/OH to R/R′ = CH_3/OH. This general dependence on steric bulk is readily explicable in terms of increased steric requirements hindering the ability of the diphosphonate ligand to bridge two metal centers. However, the dramatic effect in the R = OH series most likely results from a synergistic interaction of steric and chelate effects (vide infra).

(b) Electronic Effects. Electron-donating groups on the central carbon atom are expected to increase the ability of the coordinated diphosphonate ligand to bind calcium. However, if present at all, this electronic effect is small and is effectively masked by the steric effect noted above. Thus, the complexes with R/R′ combinations H/Cl, H/CH_3, Cl/Cl, and CH_3/CH_3 all have essentially the same K values despite the different electronegativities of H, CH_3, and Cl.

(c) Chelate Effects. Binding to calcium by a coordinated diphosphonate can occur not only through the PO_3 groups but also through appropriate R groups. This additional bonding mode converts the diphosphonate ligand from a bidentate–bidentate bridge to a bidentate–tridentate bridge and is expected to enhance the calcium affinity of the coordinated diphosphonate. The two potentially chelating R groups investigated in this work are NH_2 (and $N(CH_3)_2$) and OH. In line with the low affinity of nitrogen ligands for calcium(II), when R = NH_2 or $N(CH_3)_2$ there is only a slight increase in the calcium affinity of the resulting diphosphonate complex, even though at pH 10 these groups are not protonated and are capable of binding to calcium. The magnitude of this slight increase is about the same as noted above for the steric and electronic effects. Thus the data do not definitively establish that the NH_2 group participates in calcium binding. However, when R = OH the exceptionally high binding constant of the HMDP complex (R/R′ = OH/H) provides strong evidence for the participation of the OH group in the calcium binding of this complex. In addition, the relatively high binding constants of the complexes with R/R′ = OH/CH_3, OH/phenyl, and OH/*tert*-butyl imply that in these complexes the OH group also binds to calcium. The dramatic drop in calcium affinity on going from the complex with R/R′ = OH/H to the substituted complexes (R = OH, R′ = CH_3, phenyl, and *tert*-butyl) indicates that the additional alkyl groups specifically interfere with chelation of the OH group to calcium.

Technetium Radiopharmaceuticals. Several recent studies on ^{99m}Tc–diphosphonate bone agents have compared the biological properties of those three agents currently in clinical use, i.e. ^{997}Tc–MDP, ^{99m}Tc–HEDP, and ^{99m}Tc–HMDP. For example, Fogelman et al.[33] have investigated the human whole-body retention of these agents, while Francis et al.[34] have examined the uptake of these agents in an osteogenic animal model. From these results, and others, it appears that the skeletal uptake of ^{99m}Tc–diphosphonate bone agents increases in the order HEDP < MDP < HMDP. While this ordering undoubtedly results from the interplay of several biological and chemical factors, it is striking that it corresponds exactly to the ordering determined in this work for the calcium affinity or coordinated diphosphonates. This correspondence suggests that the calcium affinity of diphosphonates coordinated to technetium is an important factor in determining the biodistribution of ^{99m}Tc–diphosphonate skeletal imaging agents. Since the mechanism of action of ^{99m}Tc-diphosphonate imaging agents presumably[9,30] involves binding of the ^{99m}Tc–diphosphonate complex to calcium (either in the hydroxyapatite of bone or the amorphous calcium phosphate of myocardial infarcts), it is not unreasonable that the calcium affinity of the coordinated diphosphonate ligand should strongly influence biodistribution. Francis et al.[34] and others[9] have suggested that tridentate binding involving the hydroxyl group of the ^{99m}Tc–HEDP and ^{99m}Tc–HMDP skeletal imaging agents at the surface of bone is an important factor determining the uptake of these agents. Our results support this suggestion, with the elaboration that the extra methyl group of HEDP (relative to HMDP) significantly decreases the ability of this ligand to function as a bidentate–tridentate bridge.

Acknowledgment. Financial support by the National Institutes of Health (Grant Nos. HL-21276 and GM-27832) is gratefully acknowledged.

Registry No. $[(en)_2Co(MDP)]^-$, 84895-52-3; $[(en)_2Co(EDP)]^-$, 84895-41-0; $[(en)_2Co(DMDP)]^-$, 84895-42-1; $[(en)_2Co(HMDP)]^-$, 84895-43-2; $[(en)_2Co(HEDP)]^-$, 84895-44-3; $[(en)_2Co(PhHMDP)]^-$, 84895-45-4; $[(en)_2Co(BuHMDP)]^-$, 84895-46-5; $[(en)_2Co(AMDP)]^-$, 84895-47-6; $[(en)_2Co(AEDP)]^-$, 84895-48-7; $[(en)_2Co(Me_2NMDP)]^-$, 84895-49-8; $[(en)_2Co(ClMDP)]^-$, 84895-50-1; $[(en)_2Co(Cl_2MDP)]^-$, 84895-51-2; $[(en)_2Co(H_2MDP)]ClO_4$, 84895-54-5; $[(en)_2Co(H_2EDP)]ClO_4$, 84895-55-6; $[(en)_2Co(H_2DMDP)]ClO_4$, 84927-06-0; $[(en)_2Co(H_2HMDP)]ClO_4$, 84895-56-7; $[(en)_2Co(H_2HEDP)]ClO_4$, 84895-57-8; $[(en)_2Co(H_2PhHMDP)]ClO_4$, 84895-58-9; $[(en)_2Co(H_2BuHMDP)]ClO_4$, 84895-59-0; $[(en)_2Co(H_2ClMDP)]ClO_4$, 84895-60-3; $[(en)_2Co(H_2Cl_2MDP)]ClO_4$, 84895-61-4; $[(en)_2Co(H_3AMDP)](ClO_4)_2$, 84895-63-6; $[(en)_2Co(H_3AEDP)](ClO_4)_2$, 84895-65-8; $[(en)_2Co(H_2Me_2NMDP)](ClO_4)_2$, 84895-67-0; *cis*-$[(en)_2CoCl_2]Cl$, 14040-32-5; Ca^{2+}, 14127-61-8.

Supplementary Material Available: Listings of visible–UV spectrophotometric parameters, ^{1}H and ^{31}P NMR spectral parameters, elemental analyses, observed and calculated structure factors, anisotropic thermal parameters, root-mean-square displacements, hydrogen atom positional parameters, selected bond lengths and angles involving hydrogen atoms, and possible hydrogen-bond lengths and angles (27 pages). Ordering information is given on any current masthead page.

(33) Fogelman, I.; Tofe, A. J.; Francis, M. D. *J. Nucl. Med.* **1981**, *22*, P78.

(34) Francis, M. D.; Ferguson, D. L.; Tofe, A. J.; Bevan, J. A.; Michaels, S. E. *J. Nucl. Med.* **1980**, *21*, 1185.